Intraplacental injection of human iPSC-derived PDX1+ pancreatic progenitors prolongs Pdx1-deficient mice survival

Arata Wakimoto[1], Hyojung Jeon[1,3], Zeynab Javanfekr Shahri[1,2], Takuto Hayashi[4], Ching-Wei Liao[1,2], Natalia Gogoleva[1,2], Fabian Suchy[5], Atsushi Noda[1], Yuri An[7], Hiromitsu Nakauchi[5,6], Yohei Hayashi[7*] ,Michito Hamada[1,8*], Satoru Takahashi[1,8*]

1. Department of Anatomy and Embryology, Faculty of Medicine, University of Tsukuba, 1-1-1, Tennodai, Tsukuba, Ibaraki 305-8575, Japan.
2. Ph.D. Program in Human Biology, School of Integrative and Global Majors, University of Tsukuba, 1-1-1, Tennodai, Tsukuba, Ibaraki 305–8575, Japan.
3. Division of Cell Regulation, Center of Experimental Medicine and Systems Biology, The Institute of Medical Science, The University of Tokyo, 4-6-1 Shirokanedai, Minato-ku, Tokyo 108-8639, Japan.
4. Univ Paris Est Creteil, INSERM, IMRB, F-94010 Creteil, France.
5. Institute for Stem Cell Biology and Regenerative Medicine, Stanford University School of Medicine, Stanford, CA 94305, USA.
6. Stem Cell Therapy Laboratory, Advanced Research Institute, Tokyo Medical and Dental University (TMDU), Bunkyo-ku, Tokyo 113-8510, Japan.
7. iPS Cell Advanced Characterization and Development Team, BioResource Research Center, RIKEN, 3-1-1 Koyadai, Tsukuba, Ibaraki 305-0074, Japan.
8. Laboratory Animal Resource Center, Faculty of Medicine, University of Tsukuba, 1-1-1, Tennodai, Tsukuba, Ibaraki 305-8575, Japan.

*correspondence;
yohei.hayashi@riken.jp (Y.H.), hamamichi@md.tsukuba.ac.jp (M.H.), satoruta@md.tsukuba.ac.jp (S.T.)

Summary

Interspecies chimeras comprising human tissues have potential for use in disease modeling and regenerative medicine. Here, we successfully transplanted human induced pluripotent stem cell (iPSC)-derived PDX1+ pancreatic progenitor cells into Pdx1-deficient mouse embryos via intraplacental injection. The engrafted human cells predominantly localized to the duodenum, produced insulin, and extended the lifespan of *Pdx1*$^{-/-}$ mice by up to 10 days after birth. Transcriptomic analyses confirmed human pancreatic gene expression in human cells engrafted into the mouse duodenum. Our findings demonstrate the feasibility of generating interspecies chimeras with functional human pancreatic cells through *in utero* transplantation of lineage-committed progenitors. This approach circumvents developmental barriers while minimizing ethical concerns associated with PSCs. However, the incomplete rescue of the *Pdx1*$^{-/-}$ phenotype highlights the need for further research to enhance human cell engraftment and tissue integration. Overall, this study provides a foundation for developing human-animal chimera models for studying human development and regenerative therapies.

Introduction

Interspecies chimeras with human tissues represent a promising approach for developing human disease models and generating organs for transplantation. Successful intraspecies (mouse-mouse) (Hamanaka et al., 2018;) and interspecies (mouse-rat) (Goto et al., 2019; Kobayashi et al., 2010, 2021; Wu et al., 2017) chimeras have been established through blastocyst complementation. However, integrating functional human tissues into animal models has proven challenging (Hu et al., 2020; Maeng et al., 2021; Masaki et al., 2015; Wang et al., 2023b).

An alternative approach for generating chimeric animals is to inject tissue stem/progenitor cells into a developing embryo using *in utero* injections (Cohen et al., 2020; Fleischman and Mintz, 1979a; Fujiki et al., 2003; Jeon et al., 2021). Previous studies using neural crest cells successfully engrafted human cells into mouse embryos (Cohen et al., 2016, 2020). Utilizing lineage-committed cells minimizes the likelihood of donor cell differentiation for unintended purposes such as germline transmission and carcinogenesis (Crane et al., 2019; Wu et al., 2016).

Human pancreatic xenograft models are generated using newborn and adult NSG mice (Augsornworawat et al., 2020; Ma et al., 2018). These models have provided valuable insights into the functionality of human induced pluripotent stem cell (iPSC)-derived pancreatic cells *in vivo*. However, successful transplantation of human pancreatic progenitors into mouse embryos has not yet been accomplished because of the low survival rate of *in utero* injection systems.

We also developed an intraplacental injection method to deliver cells (Jeon et al., 2021) and virus vectors (Gogoleva et al., 2023) into mouse post-implantation embryos through the placenta. Fleischman and Mintz reported that intraplacental injection can transplant the mouse hematopoietic cells into anemic mouse embryos and ameliorate this phenotype (Fleischman and Mintz, 1979b). We extended this technique to conduct rat hematopoietic stem cell (HSC) transplantation into HSC-deficient mouse embryos at an embryonic day 11.5 (E11.5) and successfully engrafted xenogenic hematopoietic cells (Jeon et al., 2021). Recently, we succeeded in injecting adeno-associated virus serotype 9 at an earlier time point (E9.5) when the placental connection was established, demonstrating the transgene's broad transduction (Gogoleva et al., 2023). Because intraplacental injection does not penetrate the embryos directly, this method has a higher survival rate (80%) than other *in utero* injection methods.

Along with the placental connection established at E9.5, the initial indication of pancreas formation occurs as the dorsal endodermal epithelium thickens just below the stomach (Puri and Hebrok, 2007). All known pancreatic cell lineages originate from a small cluster of precursor cells within the foregut endoderm as defined by the expression of pancreatic and duodenal homeobox 1 (Pdx1) (Byrnes et al., 2018). *Pdx1* is recognized as a master regulator of pancreatic development, and its deficiency results in a lack of the whole pancreas and postnatal lethality within a day (Offield et al., 1996).

Various methods exist for differentiating iPSCs into pancreatic cell types, especially pancreatic β cells (Liu et al., 2014; Ma et al., 2018; Shahjalal et al., 2014). Most differentiation protocols follow a stepwise approach involving the progression of PSCs to definitive endoderm, pancreatic progenitors, and finally, functional pancreatic β cells.

Therefore, we hypothesized that introducing human iPSC-derived PDX1+ pancreatic cells into *Pdx1*-deficient mouse embryos would enable the derivation of human pancreatic tissue by occupying this vacant developmental niche. In this study, we investigated a method to generate a mouse model with human pancreatic tissue by transplanting iPSC-derived human PDX1-positive cells into *Pdx1*$^{-/-}$ mice lacking a pancreas. The resulting human-mouse chimera exhibited prolonged survival compared with that of uninjected *Pdx1*$^{-/-}$ mice. The engrafted donor-derived cells were capable of secreting human insulin. Notably, the transplanted human cells were primarily engrafted ectopically, predominantly in the duodenum. Our findings suggest that the *in utero* transplantation of lineage-committed human cells can give rise to interspecific chimeras with functional human-derived cells.

Results

Differentiation culture of human PDX1-positive cells

To conduct the intraplacental injection of human PDX1-expressing cells into *Pdx1*$^{-/-}$ mouse embryos, PDX1 expression was induced by stepwise differentiation (Figure S1A). Undifferentiated human iPSCs were maintained under feeder-free conditions. Subsequently, human iPSCs containing PDX1-P2A-tdTomato reporter were differentiated into PDX1-expressing cells by changing the differentiation medium. Endogenous PDX1 expression was confirmed by observing tdTomato on day 14 of culture (Figure 1A). As a result, 90% of the live cells expressed PDX1, demonstrating the efficiency of the differentiation culture (Figure 1A).

For easier tracking of human cells, we obtained another human iPSC line with constitutive expression of the using the EEF1A1-iRFP670 transgene. To ensure stable expression after differentiation, we conducted the same differentiation culture. After differentiation, we confirmed near-infrared fluorescent protein (iRFP) expression using flow cytometry (Figure S1B). The intensity of iRFP decreased 10-fold (peaking at $10^{5.5}$ in undifferentiated cells and $10^{4.5}$ in differentiated cells).
The expression of key marker genes such as *NANOG*, *SOX17*, *HNF6*, *PTF1A*, *NKX6-1*, and *NGN3* was monitored by RT-qPCR (Figure 1B, Figure S1C). During differentiation, the pluripotency marker *NANOG* was downregulated. From days 1 to 3, the definitive endoderm genes *SOX17* and *HNF6* were upregulated. Subsequently, the pancreatic foregut genes *PDX1* and *PTF1A* were expressed. The pancreatic progenitor gene *NKX6-1* was also expressed.

RNA sequencing (RNA-seq) analysis was performed to further characterize the donor cells. A total of 11,747 differentially expressed genes (DEGs; false discovery rate [FDR] < 0.01) were identified, and principal component analysis (PCA) showed that the gene expression profiles were completely separated before and after differentiation (Figure S2A). Genes associated with pancreatic development were upregulated in differentiated cells (Figure 1C, Figure S2B), whereas the pluripotency markers *NANOG*, *SOX2*, and *POU5F1* were significantly downregulated (Figure 1C, D, Figure S2C). Conversely, the pancreatic progenitor signature genes *PDX1*, *SOX9*, *HNF1B*, *NKX6.1*, *FOXA2*, and *HOXB4* were significantly upregulated (Figure 1C, Figure S2D). However, the pancreatic endocrine progenitor genes *NEUROD1* and *NEUROG3* were not upregulated (Figure S2E). Moreover, the pancreatic endocrine effector genes *INS*, *GCG*, *PPY*, and *SST* were not expressed (Figure 1D, Figure S2F).
Taken together, PDX1-expressing pancreatic progenitor cells were induced from human iPSC lines.

Intraplacental injection of human PDX1-positive cells does not inhibit embryonic development at low concentrations

To set the cell number for injection, we first intraplacentally injected human pancreatic cells at various concentrations into wild-type (WT) embryos (Figure 1E, F) at E10.5. Human iPSCs differentiated into PDX1-expressing pancreatic cells after 13 days of differentiation culture. On day 2 of culture, we mated the $Pdx1^{+/-}$ mice to obtain E10.5 embryos on day 13 of culture (Figure 1E). The number of embryos was counted after transplantation. After transplantation, we waited for birth and counted the number of newborns to calculate the birth rate.
The birth rate after injection was significantly lower (37, 37, 18, and 37%) at high concentrations (2×10^5 to 2.5×10^4 per embryo). On the other hand, low concentrations (1×10^4 and 5×10^3 per embryo) displayed birth rates comparable to that of the phosphate-buffered saline (PBS) injection control (>80%) (Figure 1F, Table S1). Frequent embryonic resorption has been observed in mothers with low birth rates. Therefore, we set the concentration of cells at 1×10^4 per embryo in all experiments.

Human pancreatic cells extend the lifespan of *Pdx1*$^{-/-}$ mice

Next, human pancreatic cells were intraplacentally injected into embryos obtained from $Pdx1^{+/-}$ mouse matings. We confirmed that $Pdx1^{-/-}$ mice had been born and that the genotype distribution in the newborns matched the Mendelian rule (Table S2). Uninjected $Pdx1^{-/-}$ newborns died a day after birth, as previously reported (Offield et al., 1996). On the other hand, human pancreatic cell-injected $Pdx1^{-/-}$ newborns survived up to 10 days, and their lifespans were significantly longer than those of uninjected mice ($p = 0.0013$ in the log-rank test) (Figure 2A). Thus, $Pdx1^{-/-}$ mice likely survived due to the contribution of human pancreatic cells.

In our gross observations, the long-surviving $Pdx1^{-/-}$ mice appeared small and thin compared with their WT and $Pdx1^{+/-}$ littermates, indicating that the cells could not compensate for their growth abnormality (Figure 2B, C). In addition, pancreatic structures were not observed even in long-surviving $Pdx1^{-/-}$ (Figure 2D).
Therefore, although human pancreatic cell injection into $Pdx1^{-/-}$ mice extended their lifespan, it did not correct the developmental abnormalities associated with their genotype.

Human insulin production was detected in transplanted *Pdx1*$^{-/-}$ mice

To determine whether human pancreatic cells display physiological activities, we tested the casual blood glucose levels of transplanted newborn mice daily. Of the four $Pdx1^{-/-}$ mice used for blood

glucose measurement, two did not show an increase in blood glucose and died on the third day of life. The other two mice showed increased blood glucose levels to 350 mg/dL on the fourth day of life, which decreased to below the detection limit (20mg/dL) by the sixth day. In contrast, WT mice remained stable at approximately 100 mg/dL (Figure 2E).

Next, human C-peptide in *Pdx1*$^{-/-}$ mouse serum was quantified using ELISA. On the day of birth (P0), the mice showed a maximum value of 30 pmol/L, significantly higher than that in uninjected mice (Figure 2F). In contrast, mice on P2 tended to have slightly higher values than those of uninjected mice and lower than those of P0 mice. These results demonstrated human insulin production in *Pdx1*$^{-/-}$ mice. Additionally, human pancreatic cell function has been suggested to diminish over time, owing to reduced insulin secretion or human cell number.

Human cell ectopic distribution in *Pdx1*$^{-/-}$ newborns

Although the injected pancreatic cell-deficient mice survived significantly longer, pancreatic structures in their bodies were not observed. Therefore, we attempted to determine the ectopic engraftment of human pancreatic cells. Several studies have reported that pancreatic cells can arise ectopically because of deficiencies in transcription factors essential for pancreatic development. Pancreatic endocrine cells have been observed in the spleen of *Ptf1a* knockout mice (Krapp et al., 1998). In addition, pancreatic cells have been found in the stomach, duodenum, and bile duct of *Hes1* knockout mice (Fukuda et al., 2006).

Among the various DNA quantification methods, we selected droplet digital PCR (ddPCR) to assess human pancreatic cell ectopic distribution. ddPCR enables absolute DNA quantification by partitioning PCR products into numerous tiny droplets. A previous study demonstrated its utility for chimerism quantification (Suchy et al., 2022). We established a human DNA quantification system using a combination of probes targeting primate-specific (*Caspase7*) and conserved mammalian sequences (*Zeb2*) (Suchy et al., 2024). As a positive control, we mixed human DNA from human iPSCs and mouse DNA from WT mouse blood at a known ratio. As a result, ddPCR yields the precise ratios of human DNA in the samples (0, 1, 10, 50, and 100%) (Figure S3A,B).

We measured the human DNA ratio in various organs, including the truncated pancreas, kidney, intestine (other than the duodenum), liver, lungs, and spleen. Among the organs measured, only the duodenum had a significantly higher proportion of human DNA than the uninjected samples. The duodenum showed the highest percentage of human DNA, at most 2.8% (Figure 3A).

Verification of human cell ectopic engraftment in *Pdx1*$^{-/-}$ newborns

Next, we performed flow cytometric analysis to detect human cells in the duodenum. We detected CD45.2 and CD31 double-negative, transgenic human cell marker iRFP, and human leukocyte antigen (HLA) double-positive populations in the transplanted samples (Figure 3B). In the injected duodenum, these populations were 6% on average and significantly more frequent than those in the uninjected controls. This result further confirms the ectopic engraftment of human cells in the duodenum.

We then performed immunohistochemical (IHC) confirmation using anti-human nuclear staining. Consistent with ddPCR detection, nuclear staining was observed in the duodenal villi (Figure 3C). Moreover, INS and HuNu double-positive cells were observed in the duodenum. These INS/HuNu

double-positive cells were not observed in the uninjected duodenum. Based on these results, human pancreatic cells transplanted by intraplacental injection were shown to engraft and function as pancreatic β cells in the duodenum.

Flow cytometric analysis also detected iRFP single positive cells (peaked at 4.8%, 1.5% on average) in the spleen of injected *Pdx1*$^{-/-}$ mice (Figure S4A). However, these cells were not HLA-positive. To determine if there were intact human cells, immunohistochemistry was performed on the human nuclei in the spleen. HuNu staining did not co-localize with DAPI in the spleen (Figure S4B). We confirmed that anti-human nuclei antibody excellently stains human cell nuclei *in vitro* (human iPSCs) and *in vivo* (human teratoma generated in NSG mice femur) and does not stain mouse skeletal muscle (Figure S5A,B), suggesting that the iRFP-positive spleen cells were not human cells.

Single-cell RNA-seq was performed on cells sorted from the spleen using iRFP fluorescence. All clusters were annotated as splenocytes, including B cells, macrophages, and erythrocytes (Figure S4C). These data further suggest that the iRFP-positive cells in the spleen are not intact human cells.

Human pancreatic cells in the mouse duodenum express pancreatic genes

To determine whether human cells in the duodenum of *Pdx1*$^{-/-}$ mice express pancreatic genes, we conducted RNA-seq analysis of the duodenum with or without injection. Because the injected samples could be chimeric, the reads were separated into human- or mouse-derived. To separate human and mouse reads from chimeric tissue, we first mapped the reads onto the human genome (hg38) without allowing any mismatches, and the mapped reads were treated as human reads. Subsequently, the reads were mapped onto the mouse genome (mm10) without any mismatches (Figure S6A) and collected as mouse reads. Gene expression analyses were performed separately for human and mouse reads.

PCA of human gene expression showed a clear separation of gene expression profiles between the injected and uninjected samples (Figure 4A). A total of 83 genes were upregulated, showing more than 4-fold expression (Log2foldchange > 2, p-adj < 0.05) (Figure 4B, red dots).

Genes related to endocrine pancreas development (Figure 4C), insulin secretion (Figure 4D and Figure S6B), exocrine pancreas development (Figure 4E), and pancreas development (Figure S6C) were assessed in donor cells and uninjected and injected duodenums. Among these gene sets, *BMP4*, *INSM1*, *HES1*, *KLF7*, *PPP3B*, *EFNA5*, *EPHA5*, *SFRP1*, *ISL1*, *PRKCB*, and *SYTL4* showed robust upregulation in the injected samples. In injected samples 7, 8, 9, and 10, gene subsets were upregulated, including *NKX6-1, NKX6-2, NKX2-2, MAFA, GCG, NOS2*, and *PDX1d*. The specific upregulation of these genes in a sample subset suggests heterogeneity in the differentiation status of transplanted human cells, with some cells potentially acquiring a more mature pancreatic endocrine cell phenotype.

These results support the presence of human pancreatic cells in the duodenal samples of transplants. These cells maintain pancreatic cell characteristics within the duodenum and may differentiate towards β cells. However, *INS* expression was not detected in our RNA-seq dataset, and RT-qPCR of human *INS* using the same RNA samples did not confirm *INS* mRNA (Figure 4F). We also identified several insulin secretion-related genes that were not upregulated (Figure S6B).

Furthermore, mouse reads were analyzed. PCA analysis of mouse genes suggested a change in the gene expression profile due to human pancreatic cell injection (Figure S7A). A total of 627

upregulated and 70 downregulated genes were observed (Figure S7B). The Gene Ontology (GO) terms for the upregulated genes included epithelial cell functions, including skin-related processes and gastric acid secretion. On the other hand, the downregulated genes included those involved in the positive regulation of inflammation. These results suggested that gene expression in mouse cells changes in response to human cell engraftment.

In summary, human pancreatic endocrine genes were upregulated, and mouse cells upregulated epithelial cell development genes. Overall, these findings provide evidence of the engraftment and survival of human pancreatic cells in the mouse duodenum.

Discussion

Our study demonstrated the first successful transplantation of human iPSC-derived pancreatic progenitor cells into mouse embryos. Transplanted human cells engrafted into the mouse developmental environment maintain the expression of pancreas-related genes and differentiate into insulin-producing cells. These results demonstrated the potential of the mouse environment to support human cell differentiation and functional maturation. Moreover, the transplantation of human pancreatic cells extended the lifespan of *Pdx1*$^{-/-}$ mice by up to 10 days, compared with the one-day lifespan of untreated knockouts, highlighting the ability of human cells to support host development and function.

The present study used *Pdx1*$^{-/-}$ mice as a model for evaluating postnatal human pancreatic cell function, which is yet to be performed in blastocyst injection experiments owing to ethical and technical difficulties. Recently, the survival rate of human iPSCs in animal embryos has been increased by inducing a naïve state and making them resistant to apoptosis through *BCL2* overexpression and *TP53* knockout (Wang et al., 2023a, 2023b; Zheng et al., 2021; Zhu et al., 2022). However, because most chimeric animal embryos are created using blastocyst injection, postnatal functional evaluation is inaccessible owing to technical and ethical restrictions. In contrast, our experimental system allowed us to evaluate the function of human cells after birth, which is an advantage over previous studies. Previous studies by Cohen et al. demonstrated the transplantation of human neural crest cells and induction of pigmentation in newborn WT mice by their introduction into amniotic fluid (Cohen et al., 2016). The present study showed that differentiated human cells can be engrafted using *in utero* transplantation. Our study further demonstrated that human cells are functional after *in utero* transplantation by confirming their survival in *Pdx1*$^{-/-}$ mice.

The detection of human insulin production and the presence of insulin-positive human cells within the duodenum of transplanted mice provide evidence of the functional capacity of the engrafted cells. The ddPCR analysis revealed that the duodenum contained the highest percentage of human DNA, reaching up to 2.8%. IHC staining confirmed the presence of insulin-positive human cells in the tissue. RNA-seq analysis showed that the donor cells did not express endocrine cell marker genes before transplantation and showed a pancreatic progenitor gene expression pattern. On the other hand, RNA-seq analysis revealed that the expression of genes related to the endocrine pancreas and insulin secretion, such as *ISL1*, were upregulated in some transplanted samples. This suggests that human pancreatic progenitors ectopically engrafted in the duodenum may have differentiated into endocrine cells and acquired an insulin-secreting capacity during mouse development. However, the expression of *INS* mRNA was not detected in the RNA-seq dataset nor confirmed by RT-qPCR, and several insulin secretion-related genes were not upregulated. Additionally, serum C-peptide levels were reduced in the P2 samples. This may be because of the differentiation state of the transplanted human

cells or the environment in the mouse body, which is unsuitable for insulin expression and production. This may have resulted in the timing of *INS* mRNA expression not matching that at P0 when sampling was performed.

In mice, insulin production occurs in two distinct phases. The first wave commences on E11.5, followed by a substantial increase in insulin accumulation at E15.5 (Prasadan et al., 2002). Insulin protein is synthesized in β-cells as preproinsulin and then immediately converted to proinsulin, stored in exosomes until secretion. Several studies have suggested that proinsulin and insulin reside in storage depots for days before release or degradation (Halban, 1991). Therefore, despite the detection of C-peptide in the serum of transplanted mice at P0 and the identification of insulin-positive cells in the duodenum, *INS* mRNA was not detected because it may initiate insulin production before the day of birth (P0) and subsequently lose this capability by P0. This process may involve a host rejection mechanism. Our previous and current studies using intraplacental injection suggested that xenogeneic cells were not immediately eliminated from the mouse fetus (Jeon et al., 2021). However, rejection by the innate immune system may occur, and/or postnatal adaptive immunity may be activated by the synthesis of new human proteins after cell differentiation. Since no immunological intervention was used in the current study, further studies are needed to determine whether immunodeficient mice promote the survival of human cells.

How transplanted human cells migrate to the duodenum remains a topic for future research. However, islet cells are less dependent on the engraftment site and have been used in various ectopic transplantations (Cayabyab et al., 2021). Our results suggest that the duodenum may be a valid target site for transplanting pancreatic endocrine cells. Because the duodenum expresses Pdx1 (Offield et al., 1996), it may provide a preferable environment for PDX1-positive cells under pancreatic deficiency. Considering that pancreatic cells are found in the stomach, duodenum, and bile duct of *Hes1* knockout mice (Fukuda et al., 2006), epithelial cells in the digestive tract may share a differentiation trajectory with pancreatic cells and provide a preferable environment for ectopic pancreatic cells. Further research is required to understand how human cells migrate and settle in the body, including data on the changes in the distribution and number of human cells over time after transplantation.

We found that intraplacental injection of lineage-committed cells is an alternative approach for generating interspecies chimeras in distant species. Since using progenitor cells diminishes the potential technical and ethical concerns of iPSCs, such as creating germ cells and affecting comprehensive capability, it can provide a safer and more accessible human-animal chimera research method. A previous study by Ma and colleagues established a xenotransplantation model of human pluripotent stem cell-derived pancreatic β-like cells in the newborn mouse pancreas (Ma et al., 2018). However, *in utero* injection of pancreatic progenitor cells has not yet been achieved. Using our intraplacental injection system, we accomplished stable injection with an 80% survival rate of injected fetuses. This high survival rate after intraplacental injection overcomes previous limitations, and we succeeded in delivering embryos with stable cell transplantation. Future transplantation experiments with different donor cell-recipient animal combinations will enable the integration of various cells into the developing embryo.

Intraplacental injection of human tissue progenitor cells is a new method for human-animal chimera research, allowing for the functional integration of human cells into mice. The current study is expected to contribute significantly to future research on generating human disease models and organ transplantation. However, it is essential to note that long-surviving *Pdx1*$^{-/-}$ mice remained small and thin compared with their littermates, and pancreatic structures were not formed. These results indicate

that human pancreatic cells can partially support the survival of *Pdx1*$^{-/-}$ mice but are insufficient to fully compensate for their lethality. In addition, the variability in gene expression between samples may reflect differences in transplantation success and engrafted cell viability and the stability of their phenotype after transplantation. Understanding the factors influencing transplantation success and engrafted cell phenotype stability is crucial for developing effective cell replacement therapies for diabetes using interspecies chimeras. In addition, the fact that no genes associated with exocrine cell development were identified suggests a limitation in the differentiation potential of donor cells. Generating chimeric mice with more prolonged survival may be possible by changing the recipient to *Ngn3*$^{-/-}$, which lacks only endocrine cells in the pancreas (Gradwohl et al., 2000).

Human-animal chimeras have immense potential for human disease modeling, drug screening, and organ transplantation. However, robust generation of functional and integrated human tissues in animals is difficult. To achieve *in vivo* organ generation in the future, studying the mechanisms by which human cells are rejected from animal embryos and developing strategies for efficiently transplanting human donor cells into animal embryos is essential. Previous studies have shown that the innate immune system plays an essential role in xenotransplantation (Azimzadeh et al., 2015; Chen, 2021; Ide et al., 2007) and that the contribution of human cells can be increased by suppressing their apoptosis (Zheng et al., 2021). However, as shown in the current study, phenomena caused by distant interspecies chimerism, such as developmental abnormalities caused by the injection of an excess number of human cells, are poorly understood. In future studies, investigating the mechanisms underlying the elimination of human cells by mouse embryos and developing strategies to overcome these obstacles will be imperative.

Experimental Procedures

Animals

WT B6D2F1 (BDF1) mice were obtained from The Jackson Laboratory, Yokohama, Japan. *Pdx1-LacZ* heterozygous (*Pdx1*$^{+/-}$) mice (Offield et al., 1996) were crossed with BDF1 mice for more than 10 generations to generate hybrids, as the better proliferation of hybrid strains was preferable. All mice were maintained under specific pathogen-free conditions at the University of Tsukuba Laboratory Animal Resource Center. All experiments were performed under relevant Japanese and institutional laws and guidelines and were approved by the University of Tsukuba Animal Ethics Committee (authorization number 23–039).

Genotyping

Genotypes were determined by PCR analysis of tail DNA. For genotyping, the primers for *Pdx1* loci were as follows: Pdx1_FW 5′-ATTGAGATGAGAACCGGCATG-3′, Pdx1-LacZ_FW 5′-TGTGAGCGAGTAACAACC-3′, and Pdx1_RV 5′-TTCATGCGACGGTTTTGGAAC-3′. *Pdx1*$^{-/-}$ embryos, the transplantation recipients, were obtained by mating *Pdx1*$^{+/-}$ mice. The presence of a vaginal plug was checked the morning following mating, and the mice were considered to be carrying E0.5 embryos.

Generation of PDX1-tdTomato and EEF1A1-iRFP670 iPS lines using genome editing technology

The PDX1-tdTomato and EEF1A1-iRFP670 iPS lines were generated using genome editing technology modified from our method published in a previous study (Nakade et al., 2023). Briefly, the expression vector for Cas9 nuclease and the guide RNA for cleaving the *PDX1* gene (RDB20280: pX330-PDX1) were constructed by inserting annealed synthetic oligomers (5′ -CACCgcagctcctgcctctcatcg-3′ and 5′ -AAACcgatgagaggcaggagctgc-3′) into the Bbs I site of pX330-U6-Chimeric_BB-CBh-hSpCas9 vector (#42230; Addgene, Watertown, MA, USA; a gift from Prof. Feng Zhang). To construct the donor vector, a part of the human *PDX1* gene corresponding to 1 kb up- and downstream of the stop codon was amplified by PCR using a primer set (PDX1_LAf: 5′ -actgcaggttgcacccattcgcagg-3′ and PDX1_RAr: 5′ -gccttgcaagatgttctcttcctcag-3′) and genomic DNA from WI38 cells as a template. The PCR product was cloned into the KpnI site of the pCRtk2×2NN vector (RDB18670) to generate pCRtk-PDX1 using an In-Fusion HD Cloning Kit (639648; Takara Bio Inc., Shiga, Japan). Subsequently, pCRtk2X2-PDX1 was amplified into two fragments by PCR using two primer sets (PDX1 LAr and p15AoriF and PDX1 RAf and p15AoriR). To prepare the reporter-selection marker, a part of the pUC-TEZ vector (RDB18672) harboring the 2A-tdTomato and EF1 alpha promoter-driven bleomycin resistance gene was amplified by PCR using the 2Af-1-16 and Bleo-R inf-puro primer set. PCR fragments were subjected to In-Fusin cloning to generate pUCtk-PDX1-TbsdEZ (RDB20281). The DNA sequences of all constructed plasmids were confirmed using a 3500 Genetic Analyzer (Applied Biosystems, Foster City, CA, USA).

To generate the EEF1A1-iRFP670 iPSC line, the expression vector for Cas9 nuclease and the guide RNA for cleaving the EEF1A1 gene, previously described as pX459-gEEF1A1 (RDB19570 deposited in the RIKEN DNA bank) (Nakade et al., 2023). The methods for constructing the donor vector for iRFP670 insertion were the same as those for PDX1-tdTomato, described previously. The iRFP670 sequence was cloned into pNLS-iRFP670 (#45466; Addgene) (Shcherbakova and Verkhusha, 2013). The resulting vector, pCRtk-EEF1A1-iRFP670-BSD (RDB20282), was used as the donor vector.

To generate knock-in cells, 5 μg of the donor vector and 1 μg of the Cas9-gRNA expression vector were introduced into 1×10^6 cells of 1383D6 human iPSCs using an electroporator (NEPA21; Neppa Gene Co., Ltd., Chiba, Japan). Four days after electroporation, the electroporated cells underwent zeocin selection at 2 μg/mL. Since HSV-tk expression cassettes, designed outside left and right homology arms, were included in the donor vector, 30 μg/mL of ganciclovir was used to exclude clones with random insertions.

For the single-cell-derived colony cloning of PDX1-tdTomato clones, antibiotic-resistant cells were expanded to 100 cells/cm^2 to isolate single-cell-derived colonies. Thirty-six isolated clones were examined for the presence of targeted insertion by PCR using PDX1_SeqUpLA: 5′ -ATTTGCTGGCTCTCAGGTTGGGACT-3′ and PDX1_seqRA: 5′ -GTTGAAGCCCCTCAGCCAGGAGCAG-3′ . All 36 clones tested positive for the targeted insertion. For further experiments, we selected one clone as the PDX1-TEZ line, which was deposited in the RIKEN Cell Bank as HPS4904. For the single-cell-derived colony cloning of the EEF1A1-iRFP670 line, antibiotic-resistant and iRFP670-fluorescence-positive cells were expanded to 100 cells/cm^2 to isolate single-cell-derived colonies. Twelve Isolated clones were examined for the presence of targeted insertion by PCR using EEF1A1-up_FW: 5′ -ACATGCTGGAGCCAAGTGCTA -3′ and EEF1A1-down_Rv: 5′ -

ATCACACAAACAGAAAGCATGTCC -3′ . Eleven of the 12 clones were positive for targeted insertion. For further experiments, we selected one clone as the EEF1A1-iRFP670-TEZ line, which was deposited in the RIKEN Cell Bank as HPS5065.

Human iPSC culture and donor cell preparation

Undifferentiated human iPSCs of the PDX1-TEZ (HPS4904 in the RIKEN Cell Bank) and EEF1A1-iRFP670 (HPS5065 in the RIKEN Cell Bank) lines were maintained in feeder-free Stemfit AK02N medium (AK02N; Ajinomoto, Tokyo, Japan) to which iMatrix-511 (NP892-012; Nippi, Inc., Tokyo, Japan) and Y-27632 (Y0503; Sigma-Aldrich, St. Louis, MO, USA) were added 24 h after passage.

The culture medium used for the differentiation of PDX1-expressing cells comprised penicillin/streptomycin (P4333; Sigma-Aldrich) added to a basal medium (Stemfit or Improved Minimum Essential Medium [IMEM]). On day 0, human iPSCs were seeded at 2,500 cells/cm^2 in Stemfit AK02N supplemented with iMatrix-411 (0.25 µg/cm^2, NP892-041; Nippi, Inc.), iMatrix-511 (0.25 µg/cm^2), and Y-27632 (10 µM). On day one, the medium was replaced by Stemfit AK02N (A + B) supplemented with CHIR99021 (3 µM, #72052; STEMCELL Technologies, Vancouver, BC, Canada) and ActivinA (10 ng/mL) (725748-11-8; Fujifilm Wako Pure Chemical Corporation, Osaka, Japan). On day three, the medium was replaced by Stemfit AK02N (A + B) supplemented with activin A (10 ng/mL). On day 5, the medium was changed to Modified IMEM with L-glutamine (A1048901; Thermo Fisher Scientific, Waltham, MA, USA) supplemented with B-27 (1% v/v, 17504044; Thermo Fisher Scientific), retinoic acid (2 µmol/L, R2625; Sigma-Aldrich), cyclopamine-KAAD (0.25 µmol/L, #20943; Cayman Chemical Company, Ann Arbor, MI, USA), SB4315422 (10 µM, #72232; STEMCELL Technologies), and DMH-1 (10 µM, 4126/10; R&D Systems, Minneapolis, MN, USA). Shortly before injection, the differentiated cells were dissociated using Accutase (12679-54; Nacalai Tesque, Kyoto, Japan) for 15 min at 37°C and washed in PBS twice. The cells were then suspended in cold PBS.

Intraplacental injection

Intraplacental transplantation followed prior protocols (Jeon et al., 2021). Briefly, glass tubes were used to craft the injection needles, which were then refined to a 50-µm diameter using a grinder. Pregnant mice bearing E9.5 embryos were anesthetized with isoflurane while resting on a 37°C heating plate. The surgical procedure involved careful exposure of the uterine area through an abdominal incision. The donor cell suspension was loaded into the injection needle through mouth pipetting and subsequently affixed to a microinjector (FemtoJet; Eppendorf, Hamburg, Germany). Each placenta was punctured by an injection needle to a depth of 2 mm, and the donor cell suspension was introduced at an injection pressure of 60 hPa. After transplantation, the uterus was carefully repositioned, and the incision was securely closed. After surgery, the mice were placed in plastic bags and heated in water to prevent hypothermia.

Survival analysis

Individual identification of newborn mice was established by tattooing their limbs on the day of birth. Genotyping was performed using tail-tip samples. Maternal care was enhanced by supplementing the maternal diet with CMF sprouts (Oriental Yeast; Tokyo, Japan). Newborn survival was checked daily postpartum until all *Pdx1*$^{-/-}$ mice died. The Kaplan–Meier curve was constructed using GraphPad PRISM 6 (GraphPad Software, La Jolla, CA, USA).

Glucose measurement

A small amount of blood was collected daily via facial vein puncture. Blood glucose levels were measured using a glucometer (Terumo, Tokyo, Japan).

Reverse transcription-quantitative PCR

Total RNA was collected using an Isogen Kit (Cat. No. 311-02501; Nippon Gene, Tokyo, Japan). cDNA was synthesized using a QuantiTect Reverse Transcription Kit (Cat. No. 205313; Qiagen, Hilden, Germany). Gene expression levels were determined using RT-qPCR performed on a Thermal Cycler Dice Real Time System Single TP850 (Takara Bio Inc.) using THUNDERBIRD® SYBR® qPCR Mix (QPS-201; TOYOBO Co., Ltd., Tokyo, Japan). mRNA levels were normalized to those of RPLP0. The primer sequences used were summarized in Table S4.

RNA sequence analysis of human iPSC differentiation

Total RNA was extracted using TRIzol (Thermo Fisher Scientific) following standard protocols. An RNA-seq library was prepared using an NEBNext Ultra II Directional RNA Library Prep Kit (New England Biolabs, Ipswich, MA, USA) after ribosomal RNA (rRNA) depletion using an NEBNext rRNA Depletion Kit (New England Biolabs). Paired-end (2 × 36 bases) sequencing was performed using a NextSeq500 platform (Illumina, San Diego, CA, USA). The FASTQ files were imported into the CLC Genomics Workbench (version 10.1.1; Qiagen), and the sequence reads were mapped to the human reference genome (hg38). Gene expression was calculated as the total read count normalized to transcripts per million.
DEGs were extracted using the criterion of FDR-corrected $p < 0.05$. PCA plots were constructed using Python software.

RNA sequence analysis of chimeric duodenum

Paired-end (2 × 36 bases) sequencing was performed using the same protocol for the iPSC differentiation experiment. FASTQ files were imported into STAR 2.7.11b. Sequence reads were mapped onto the human (hg38) or mouse reference genome (mm10) without allowing a single mismatch (--outFilterMismatchNmax 0) or multimapping (--outFilterMultimapNmax 1). DEGs were extracted using DESeq2 in R (Love et al., 2014) using the criteria of $p < 0.05$ and log2foldchange > 2. Human genes upregulated in the uninjected samples were considered contaminated mouse reads and were not subjected to analysis. GO analysis was performed using clusterprofiler (Wu et al., 2021) and the ReactomePA package(Yu and He, 2016). Gene lists were obtained from molecular signatures database at GSEA website. PCA and dot plots and clustering heatmaps were constructed using Python software.

Flow cytometric analysis

The FACS analyzers CytoFLEX (Beckman Coulter, Brea, CA, USA) and MoFlo XDP sorter (Beckman Coulter) were used. CytoExpert (Beckman Coulter) and FlowJo software (TreeStar Inc., Ashland, OR, USA) were used to analyze the data. The duodenum of newborn mice was dissociated using collagenase type V (032-17854; FUJIFILM Wako Pure Chemical Corporation) following a published protocol (Uniken Venema et al., 2022). The spleens of transplanted mice were isolated, homogenized using microscope slides (Matsunami Glass Ind., Ltd., Osaka, Japan), and treated with ACK lysis buffer. The antibodies used are summarized in Table S3.

Immunohistochemistry

Tissues were fixed in Mildform 10N (133-10311; FUJIFILM Wako Pure Chemical Corporation) and paraffinized. Paraffinized tissue blocks were sliced at a 4-μm thickness using a Sliding Microtome SM2000R (Leica Biosystems, Wetzlar, Germany) and processed for IHC staining. Antigen retrieval (S1699; Agilent Technologies, Santa Clara, CA, USA) was used and incubated with the sample for 10 min at 110°C. After blocking with 5% goat serum/1% bovine serum albumin/PBS and Mouse on Mouse blocking reagent (Vector Laboratories, Newark, CA, USA), the samples were incubated with primary antibodies overnight at 4°C. All immunostained samples were visualized using the appropriate fluorophores. Tissue sections were mounted using VECTASHIELD Vibrance Antifade Mounting Medium (Vector Laboratories). All samples were observed under a BIOREVO BZ-X800 microscope (Keyence, Osaka, Japan). All images were adjusted using Lightroom (Adobe, San Jose, CA, USA) and quantified using ImageJ software (NIH, Bethesda, MD, USA).

ELISA assay

ELISA was conducted using a Mercodia Ultrasensitive C-peptide ELISA kit (#10-1141-01; Mercodia, Uppsala, Sweden). Briefly, calibrator, control, and sample volumes of 100 μL each were added to their respective wells. Samples were prepared by diluting serum from transplanted *Pdx1*$^{-/-}$ mice. Thereafter, the plate was incubated on a shaker for 1 h at 25°C and then washed. Subsequently, 200 μL of the enzyme conjugate solution was added to each well, with another 1-h incubation on the plate shaker at room temperature. Afterward, the plate was rewashed, and 200 μL of TMB substrate was added to each well, followed by a 30-min incubation on the bench at room temperature. Next, 50 μL of stop solution was mixed into each well. Optical density readings were obtained at 450 nm, and the calculation of the results was completed within 30 min.

Single-cell RNA sequencing

For single-cell RNA sequencing (scRNA-seq), Chromium Next GEM Single Cell 3′ Reagent Kit v3.1 (PN-10000128; 10X genomics, Pleasanton, CA, USA) was used. Briefly, Gel beads-in-EMulsion (GEMs) were generated by combining barcoded Single Cell 3′ v3.1 Gel Beads, a master mix combining reverse transcription reagents, cells, and partitioning oil on a Chromium Next GEM Chip G. These gel beads incorporated a poly dT primer, facilitating the generation of barcoded full-length cDNA from polyadenylated mRNA. Following incubation, GEMs were disassembled, and the pooled fractions were recovered. Silane magnetic beads were used to purify first-strand cDNA from the post-GEM-RT reaction mixture, which included residual biochemical reagents and primers. Barcoded full-length cDNA was amplified using PCR to produce sufficient mass for library construction. After amplification, cDNA was fragmented, and sample indexes were integrated via PCR. Finally, fragment size and concentration were verified using an Agilent TapeStation (Agilent Technologies). The constructed library was shipped to Macrogen (Tokyo, Japan) without interrupting the cold chain used for sequencing.

ddPCR analysis

For ddPCR analysis, a QX200 Droplet Digital PCR system (Bio-Rad Laboratories, Hercules, CA, USA) was used. Briefly, to prepare DNA, tissue lysis was conducted in 10% proteinase K solution in a 1% SDS buffer. The samples were incubated at 55°C overnight. The following morning, another round of lysis buffer was added, and incubation was continued for a few additional hours. Proteinase K inactivation was accomplished at 75°C for 10 min, followed by extraction of 50 μL from each

sample. To precipitate SDS, 5 μL of 1 M KCl was added, and the samples were briefly centrifuged at 3,000 × *g* for 1 min at 4°C. The reaction mixture was prepared using a custom ddPCR assay (#10031276 for FAM and #10031279 for HEX; Bio-Rad Laboratories) and ddPCR Supermix for Probes (no dUTP) (#186-3023; Bio-Rad Laboratories) according to the manufacturer's instructions. Droplet formation was performed using droplet generator oil (#186-3005; Bio-Rad Laboratories). The subsequent PCR reaction involved enzyme activation at 95°C for 10 min, denaturation at 94°C for 30 s, and annealing/extension at 60°C for 1 min. This PCR cycle was repeated 50 times, and enzyme deactivation was achieved at 98°C for 10 min, with a final holding step at 12°C. QuantaSoft software (Bio-Rad Laboratories) was used to quantify the absolute number of DNA copies in all wells for data acquisition and analysis.
The sequences of primers and probes used are as follows:
chCasp7:
Fw-GAAGAAGAAAAATGTCACCATGCG, Rv-TTTCAAAATTCATGTTGTACTGATATGTAG, Probe-AGACCACCCGGGACCGAGTGCCT
Zeb2:
Fw-GGATGGGGAATGCAGCTCTT, Rv-AGTGCGGCAGAATACAGCA, Probe-TGATGGGTTGTGAAGGCAGCTGCACCT

Statistical analysis

Statistical analyses were performed using GraphPad PRISM 6 software. The statistical significance of the differences between two groups was determined using Welch's *t*-test. The statistical significance of the differences between three or more groups was determined using one-way ANOVA followed by Tukey–Kramer's multiple comparisons. The statistical significance of survival time was determined using the log-rank test. The statistical significance of the FACS analysis was determined using Fisher's exact test, with uninjected samples as background signals. Statistical significance was considered at $p < 0.05$.

Resource availability

Lead contact

Michito Hamada, Ph.D., Department of Anatomy and Embryology, Faculty of Medicine, University of Tsukuba, 1-1-1 Tennodai, Tsukuba 305-8575, Japan; Phone: +81-298-53-7516, Fax: +81-298-53-6965, E-mail: hamamichi@md.tsukuba.ac.jp

Materials availability

This study did not generate new unique reagents.

Data and code availability

RNAseq data was deposited as accession number DRR545160-DRR545181.

Supplemental information

Supplemental information can be found online at (URL)

Acknowledgments

We thank Dr. Yoshihiro Miwa, Dr. Koji Nakade, Dr. Kenichi Nakashima, and Mrs. Yasuko Hemmi for their technical support in generating PDX-TEZ and EEF1A1-iRFP670 hiPSC lines. We thank Dr. Satoshi Yamazaki for providing *Pdx1*$^{LacZ/+}$ mice and technical support for the scRNA-seq analysis. We are grateful to all former and current members of the Department of Anatomy and Embryology for their support. This work was supported by JSPS KAKENHI (Grant Number JP22H04922, 23K05586, 23K18208), JST (Grant Number JPMJPF2017), AMED (Grant number 23bm1423010h0001), and Research Fellowships of Japan Society for the Promotion of Science for Young Scientists (23KJ0238).

Author contributions

Conceptualization, S.T., Y.H., M.H.; data curation, A.W.; formal analysis, A.W.; funding acquisition, S.T., A.W., H.N.; investigation, A.W., H.J., Z.J.S., T.H., C.W.L., N.G., A.N., Y.H., F.S. Y.A.; methodology, A.W., H.J., M.H., Y.H., F.S.; project administration, A.W., M.H., S.T.; resources, S.T., Y.H., H.N.; software, A.W., T.H.; supervision, S.T., M.H.; validation, A.W., H.J., Z.J.S., T.H., C.W.L., N.G., A.N., Y.H., F.S.; visualization, A.W., M.H.; writing-original draft, A.W.; writing-review & editing, A.W., H.J., Z.J.S., T.H., C.W.L., N.G., A.N., F.S., H.N., Y.H., M.H., S.T.

Declaration of interests

The authors declare no competing interests.

Declaration of generative AI and AI-assisted technologies in the writing process

During the preparation of this work, the authors used claude3 Opus in order to improve language and readability. After using this tool/service, the authors reviewed and edited the content as needed and take full responsibility for the content of the publication.

References

Augsornworawat, P., Maxwell, K.G., Velazco-Cruz, L., and Millman, J.R. (2020). Single-Cell Transcriptome Profiling Reveals β Cell Maturation in Stem Cell-Derived Islets after Transplantation. Cell Rep. *32*, 108067. .

Azimzadeh, A.M., Kelishadi, S.S., Ezzelarab, M.B., Singh, A.K., Stoddard, T., Iwase, H., Zhang, T., Burdorf, L., Sievert, E., Avon, C., et al. (2015). Early graft failure of GalTKO pig organs in baboons is reduced by expression of a human complement pathway-regulatory protein. Xenotransplantation *22*, 310–316. .

Byrnes, L.E., Wong, D.M., Subramaniam, M., Meyer, N.P., Gilchrist, C.L., Knox, S.M., Tward, A.D., Ye, C.J., and Sneddon, J.B. (2018). Lineage dynamics of murine pancreatic development at single-cell resolution. Nat. Commun. *9*, 3922. .

Cayabyab, F., Nih, L.R., and Yoshihara, E. (2021). Advances in Pancreatic Islet Transplantation Sites for the Treatment of Diabetes. Front. Endocrinol. *12*, 732431. .

Chen, J.-C. (2021). Immunological Consequences of In Utero Exposure to Foreign Antigens. Front. Immunol. *12*, 638435. .

Cohen, M.A., Wert, K.J., Goldmann, J., Markoulaki, S., Buganim, Y., Fu, D., and Jaenisch, R. (2016). Human neural crest cells contribute to coat pigmentation in interspecies chimeras after in utero

injection into mouse embryos. Proc. Natl. Acad. Sci. U. S. A. *113*, 1570–1575. .

Cohen, M.A., Zhang, S., Sengupta, S., Ma, H., Bell, G.W., Horton, B., Sharma, B., George, R.E., Spranger, S., and Jaenisch, R. (2020). Formation of Human Neuroblastoma in Mouse-Human Neural Crest Chimeras. Cell Stem Cell *26*, 579–592.e6. .

Crane, A.T., Voth, J.P., Shen, F.X., and Low, W.C. (2019). Concise Review: Human-Animal Neurological Chimeras: Humanized Animals or Human Cells in an Animal? Stem Cells.

Fleischman, R.A., and Mintz, B. (1979a). Prevention of genetic anemias in mice by microinjection of normal hematopoietic stem cells into the fetal placenta. Proc. Natl. Acad. Sci. U. S. A. *76*, 5736–5740. .

Fleischman, R.A., and Mintz, B. (1979b). Prevention of genetic anemias in mice by microinjection of normal hematopoietic stem cells into the fetal placenta. Proc. Natl. Acad. Sci. U. S. A. *76*, 5736–5740. .

Fujiki, Y., Fukawa, K., Kameyama, K., Kudo, O., Onodera, M., Nakamura, Y., Yagami, K.-I., Shiina, Y., Hamada, H., Shibuya, A., et al. (2003). Successful multilineage engraftment of human cord blood cells in pigs after in utero transplantation. Transplantation *75*, 916–922. .

Fukuda, A., Kawaguchi, Y., Furuyama, K., Kodama, S., Horiguchi, M., Kuhara, T., Koizumi, M., Boyer, D.F., Fujimoto, K., Doi, R., et al. (2006). Ectopic pancreas formation in Hes1 -knockout mice reveals plasticity of endodermal progenitors of the gut, bile duct, and pancreas. J. Clin. Invest. *116*, 1484–1493. .

Gogoleva, N., Shahri, Z.J., Noda, A., Liao, C.-W., Wakimoto, A., Inoue, Y., Jeon, H., Takahashi, S., and Hamada, M. (2023). Intraplacental injection of AAV9-CMV-iCre results in the widespread transduction of multiple organs in double-reporter mouse embryos. Exp. Anim. https://doi.org/10.1538/expanim.23-0044.

Goto, T., Hara, H., Sanbo, M., Masaki, H., Sato, H., Yamaguchi, T., Hochi, S., Kobayashi, T., Nakauchi, H., and Hirabayashi, M. (2019). Generation of pluripotent stem cell-derived mouse kidneys in Sall1-targeted anephric rats. Nat. Commun. *10*, 451. .

Gradwohl, G., Dierich, A., LeMeur, M., and Guillemot, F. (2000). neurogenin3 is required for the development of the four endocrine cell lineages of the pancreas. Proceedings of the National Academy of Sciences *97*, 1607–1611. .

Halban, P.A. (1991). Structural domains and molecular lifestyles of insulin and its precursors in the pancreatic beta cell. Diabetologia *34*, 767–778. .

Hamanaka, S., Umino, A., Sato, H., Hayama, T., Yanagida, A., Mizuno, N., Kobayashi, T., Kasai, M., Suchy, F.P., Yamazaki, S., et al. (2018). Generation of Vascular Endothelial Cells and Hematopoietic Cells by Blastocyst Complementation. Stem Cell Reports *11*, 988–997. .

Hu, Z., Li, H., Jiang, H., Ren, Y., Yu, X., Qiu, J., Stablewski, A.B., Zhang, B., Buck, M.J., and Feng, J. (2020). Transient inhibition of mTOR in human pluripotent stem cells enables robust formation of mouse-human chimeric embryos. Sci Adv *6*, eaaz0298. .

Ide, K., Wang, H., Tahara, H., Liu, J., Wang, X., Asahara, T., Sykes, M., Yang, Y.-G., and Ohdan, H. (2007). Role for CD47-SIRPα signaling in xenograft rejection by macrophages. Proceedings of the National Academy of Sciences *104*, 5062–5066. .

Jeon, H., Asano, K., Wakimoto, A., Kulathunga, K., Tran, M.T.N., Nakamura, M., Yokomizo, T., Hamada, M., and Takahashi, S. (2021). Generation of reconstituted hemato-lymphoid murine

embryos by placental transplantation into embryos lacking HSCs. Sci. Rep. *11*, 4374. .

Kobayashi, T., Yamaguchi, T., Hamanaka, S., Kato-Itoh, M., Yamazaki, Y., Ibata, M., Sato, H., Lee, Y.-S., Usui, J.-I., Knisely, A.S., et al. (2010). Generation of rat pancreas in mouse by interspecific blastocyst injection of pluripotent stem cells. Cell *142*, 787–799. .

Kobayashi, T., Goto, T., Oikawa, M., Sanbo, M., Yoshida, F., Terada, R., Niizeki, N., Kajitani, N., Kazuki, K., Kazuki, Y., et al. (2021). Blastocyst complementation using Prdm14-deficient rats enables efficient germline transmission and generation of functional mouse spermatids in rats. Nat. Commun. *12*, 1328. .

Krapp, A., Knöfler, M., Ledermann, B., Bürki, K., Berney, C., Zoerkler, N., Hagenbüchle, O., and Wellauer, P.K. (1998). The bHLH protein PTF1-p48 is essential for the formation of the exocrine and the correct spatial organization of the endocrine pancreas. Genes Dev. *12*, 3752–3763. .

Liu, H., Yang, H., Zhu, D., Sui, X., Li, J., Liang, Z., Xu, L., Chen, Z., Yao, A., Zhang, L., et al. (2014). Systematically labeling developmental stage-specific genes for the study of pancreatic β-cell differentiation from human embryonic stem cells. Cell Res. *24*, 1181–1200. .

Love, M.I., Huber, W., and Anders, S. (2014). Moderated estimation of fold change and dispersion for RNA-seq data with DESeq2. Genome Biol. *15*, 550. .

Ma, H., Wert, K.J., Shvartsman, D., Melton, D.A., and Jaenisch, R. (2018). Establishment of human pluripotent stem cell-derived pancreatic β-like cells in the mouse pancreas. Proc. Natl. Acad. Sci. U. S. A. *115*, 3924–3929. .

Maeng, G., Das, S., Greising, S.M., Gong, W., Singh, B.N., Kren, S., Mickelson, D., Skie, E., Gafni, O., Sorensen, J.R., et al. (2021). Humanized skeletal muscle in MYF5/MYOD/MYF6-null pig embryos. Nature Biomedical Engineering *5*, 805–814. .

Masaki, H., Kato-Itoh, M., Umino, A., Sato, H., Hamanaka, S., Kobayashi, T., Yamaguchi, T., Nishimura, K., Ohtaka, M., Nakanishi, M., et al. (2015). Interspecific in vitro assay for the chimera-forming ability of human pluripotent stem cells. Development 1–9. .

Nakade, K., Tsukamoto, S., Nakashima, K., An, Y., Sato, I., Li, J., Shimoda, Y., Hemmi, Y., Miwa, Y., and Hayashi, Y. (2023). Efficient selection of knocked-in pluripotent stem cells using a dual cassette cellular elimination system. Cell Rep Methods *3*, 100662. .

Offield, M.F., Jetton, T.L., Labosky, P.A., Ray, M., Stein, R.W., Magnuson, M.A., Hogan, B.L., and Wright, C.V. (1996). PDX-1 is required for pancreatic outgrowth and differentiation of the rostral duodenum. Development *122*, 983–995. .

Prasadan, K., Daume, E., Preuett, B., Spilde, T., Bhatia, A., Kobayashi, H., Hembree, M., Manna, P., and Gittes, G.K. (2002). Glucagon is required for early insulin-positive differentiation in the developing mouse pancreas. Diabetes *51*, 3229–3236. .

Puri, S., and Hebrok, M. (2007). Dynamics of embryonic pancreas development using real-time imaging. Dev. Biol. *306*, 82–93. .

Shahjalal, H.M., Shiraki, N., Sakano, D., Kikawa, K., Ogaki, S., Baba, H., Kume, K., and Kume, S. (2014). Generation of insulin-producing β-like cells from human iPS cells in a defined and completely xeno-free culture system. J. Mol. Cell Biol. *6*, 394–408. .

Shcherbakova, D.M., and Verkhusha, V.V. (2013). Near-infrared fluorescent proteins for multicolor in vivo imaging. Nat. Methods *10*, 751–754. .

Suchy, F.P., Nishimura, T., Seki, S., Wilkinson, A.C., Higuchi, M., Hsu, I., Zhang, J., Bhadury, J.,

and Nakauchi, H. (2022). Streamlined and quantitative detection of chimerism using digital PCR. Sci. Rep. *12*, 10223. .

Suchy, F.P., Karigane, D., Nakauchi, Y., Higuchi, M., Zhang, J., Pekrun, K., Hsu, I., Fan, A.C., Nishimura, T., Charlesworth, C.T., Bhadury, J., Nishimura, T., Wilkinson, A.C., Kay, M.A., Majeti, R., and Nakauchi, H. (2024). Genome engineering with Cas9 and AAV repair templates generates frequent concatemeric insertions of viral vectors. Nat. Biotech.

Uniken Venema, W.T.C., Ramírez-Sánchez, A.D., Bigaeva, E., Withoff, S., Jonkers, I., McIntyre, R.E., Ghouraba, M., Raine, T., Weersma, R.K., Franke, L., et al. (2022). Gut mucosa dissociation protocols influence cell type proportions and single-cell gene expression levels. Sci. Rep. *12*, 9897. .

Wang, H., Yin, X., Xu, J., Chen, L., Karuppagounder, S.S., Xu, E., Mao, X., Dawson, V.L., and Dawson, T.M. (2023a). Interspecies chimerism with human embryonic stem cells generates functional human dopamine neurons at low efficiency. Stem Cell Reports https://doi.org/10.1016/j.stemcr.2023.11.009.

Wang, J., Xie, W., Li, N., Li, W., Zhang, Z., Fan, N., Ouyang, Z., Zhao, Y., Lai, C., Li, H., et al. (2023b). Generation of a humanized mesonephros in pigs from induced pluripotent stem cells via embryo complementation. Cell Stem Cell *30*, 1235–1245.e6. .

Wu, J., Greely, H.T., Jaenisch, R., Nakauchi, H., Rossant, J., and Belmonte, J.C.I. (2016). Stem cells and interspecies chimaeras. Nature *540*, 51–59. .

Wu, J., Platero-Luengo, A., Sakurai, M., Sugawara, A., Gil, M.A., Yamauchi, T., Suzuki, K., Bogliotti, Y.S., Cuello, C., Morales Valencia, M., et al. (2017). Interspecies Chimerism with Mammalian Pluripotent Stem Cells. Cell *168*, 473–486.e15. .

Wu, T., Hu, E., Xu, S., Chen, M., Guo, P., Dai, Z., Feng, T., Zhou, L., Tang, W., Zhan, L., et al. (2021). clusterProfiler 4.0: A universal enrichment tool for interpreting omics data. Innovation (Camb) *2*, 100141. .

Yu, G., and He, Q.-Y. (2016). ReactomePA: an R/Bioconductor package for reactome pathway analysis and visualization. Mol. Biosyst. *12*, 477–479. .

Zheng, C., Hu, Y., Sakurai, M., Pinzon-Arteaga, C.A., Li, J., Wei, Y., Okamura, D., Ravaux, B., Barlow, H.R., Yu, L., et al. (2021). Cell competition constitutes a barrier for interspecies chimerism. Nature *592*, 272–276. .

Zhu, Y., Zhang, Z., Fan, N., Huang, K., Li, H., Gu, J., Zhang, Q., Ouyang, Z., Zhang, T., Tang, J., et al. (2022). Generating functional cells through enhanced interspecies chimerism with human pluripotent stem cells. Stem Cell Reports *17*, 1059–1069. .

Figure Legends

Fig. 1. Establishment of intraplacental injection with human iPSC-derived PDX1-positive cells. (A) Left: representative fluorescent microscopic image of differentiated human iPSC at day 13. Right: representative flow cytometric analysis of differentiated human iPSC at day 13. (B) Heatmap analysis of core pancreatic development gene expression before (n = 4) and after (n = 4) differentiation. (C) Expression levels of *NANOG*, *PDX1*, and *INS* before (n = 4) and after (n = 4) differentiation. (D) Expression time-course of *HNF6*, *PDX1*, and *NKX6.1*. Lines represent means, normalized to *RPLP0*, and the no-differentiation control (n = 3 for each time point). (E) Schematic representation of the intraplacental transplantation experiments, created with BioRender.com. (F) Birth rates of WT embryos injected with human pancreatic progenitors at various concentrations (sample numbers are shown in Table 1). iPSC, induced pluripotent stem cell; WT, wild-type.

Fig. 2. Transplantation of human pancreatic cells supports $Pdx1^{-/-}$ newborn mice through insulin secretion. (A) Survival curves of $Pdx1^{+/-}$ (left) and $Pdx1^{-/-}$ mice (right). $Pdx1^{+/-}$; no injection, n = 10; injected at E10.5, n = 11. $Pdx1^{-/-}$; no injection, n = 4; injected at E9.5, n = 11; injected at E10.5, n =14. (B) Representative macroscopic images of newborn mice. (C) Bodyweight of newborn mice. Data are shown as individuals and means. No injection; WT, n = 5; $Pdx1^{+/-}$, n = 8; $Pdx1^{-/-}$, n = 5. Injected; WT, n = 15; $Pdx1^{+/-}$, n = 25; $Pdx1^{-/-}$, n = 11. (D) Representative macroscopic images of inner organs of $Pdx1^{+/-}$ and $Pdx1^{-/-}$ mice after injection at P0. (E) Casual blood glucose levels of injected WT (n = 3) and $Pdx1^{-/-}$ (n = 4) mice. Each line shows a tested individual. (F) Serum human C-peptide levels in uninjected (n = 8), injected P0 (n = 6), and injected P2 (n = 9) $Pdx1^{-/-}$ mice. WT, wild-type.

Fig. 3. Human pancreatic cells were engrafted ectopically in the duodenum. (A) Percentage of human DNA in various organs from injected $Pdx1^{-/-}$ P0 newborns (n = 8 for all organs). (B) Representative flow cytometric plots of the duodenum of $Pdx1^{-/-}$ mice. The gate represents the iRFP/HLA double-positive fraction. The dot plot represents the percentage of iRFP/HLA double-positive cells per DAPI-negative (live) cells. No injection, n = 5, injected, n = 10. (C) Representative immunofluorescence images of the duodenum from two injected $Pdx1^{-/-}$ newborns. (D) Representative immunofluorescence images of the duodenum from $Pdx1^{-/-}$ newborns without injection. (E) Quantification of HuNu/INS double-positive cell number per field (left) and per number of DAPI-positive cells (right). Injected: 33 fields from 3 individuals. No injection: 9 fields from 1 individual. iRFP, near-infrared fluorescent protein; HLA, human leukocyte antigen.

Fig. 4. Engrafted human cells in the duodenum show pancreatic gene expression. (A) 3D PCA plot of human genes in injected (n = 10) and uninjected duodenums (n = 4). (B) Volcano plot of human genes in injected (n = 10) and uninjected duodenums (n = 4). Colored dots show differentially expressed genes (Log2FoldChange>2, p-adjusted < 0.05.) (C–E) Heatmaps of human genes related to endocrine pancreas development. Donor cells, n = 4; No injection, n = 4; Injected, n = 10. (C) Insulin secretion (D) and exocrine pancreas development (E). (F) Relative expression of human *INS* in the mRNA tested by RNA sequencing. No injection, n = 4; injected; n = 10.

Figure 1

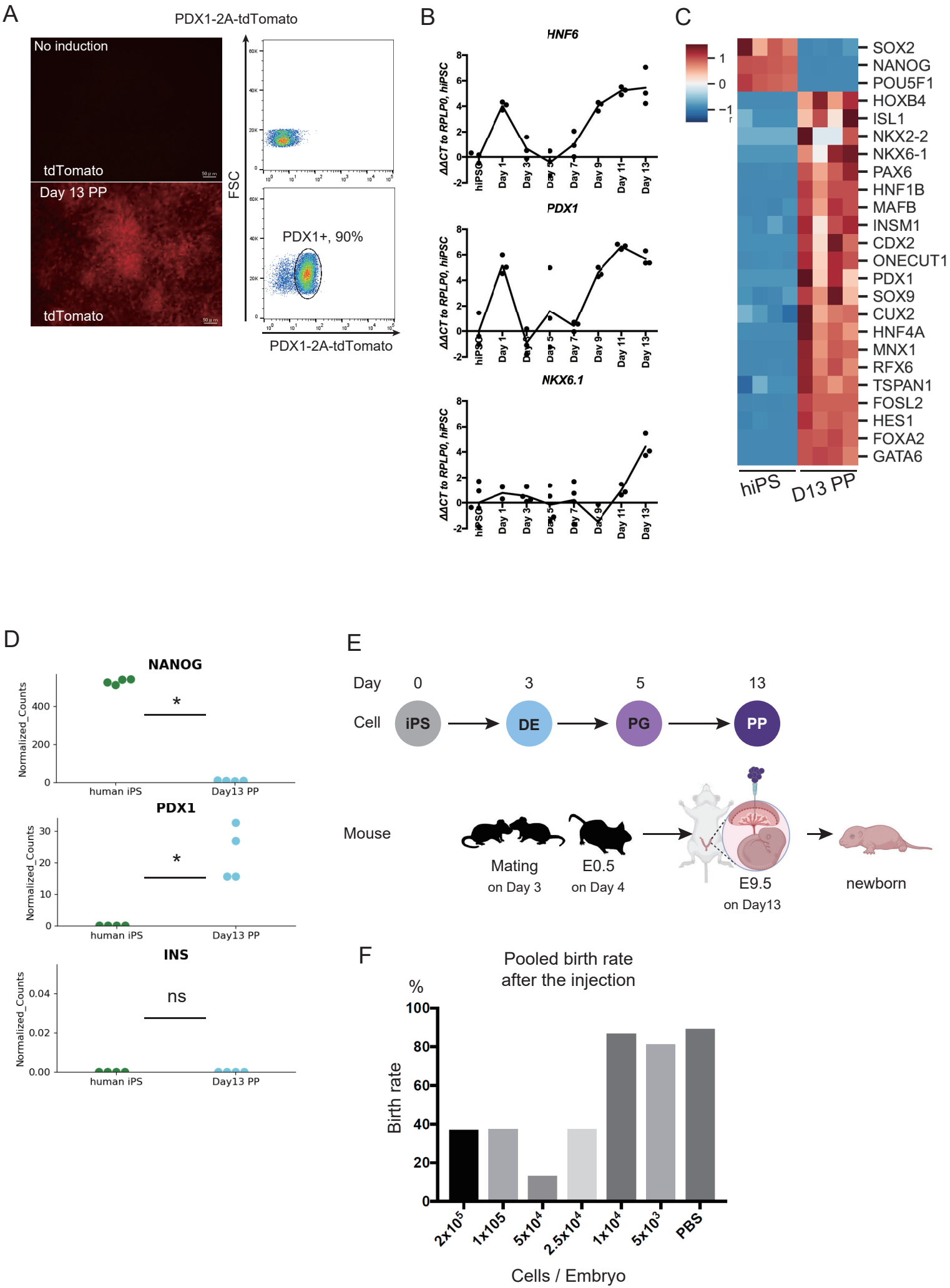
A
PDX1-2A-tdTomato
No induction
tdTomato
Day 13 PP
tdTomato
FSC
PDX1+, 90%
PDX1-2A-tdTomato
B
HNF6
PDX1
NKX6.1
ΔΔCT to RPLP0, hiPSC
hiPSC
Day 1
Day 3
Day 5
Day 7
Day 9
Day 11
Day 13
C
SOX2
NANOG
POU5F1
HOXB4
ISL1
NKX2-2
NKX6-1
PAX6
HNF1B
MAFB
INSM1
CDX2
ONECUT1
PDX1
SOX9
CUX2
HNF4A
MNX1
RFX6
TSPAN1
FOSL2
HES1
FOXA2
GATA6
hiPS
D13 PP
D
NANOG
PDX1
INS
Normalized_Counts
human iPS
Day13 PP
ns
E
Day
0
3
5
13
Cell
iPS
DE
PG
PP
Mouse
Mating
on Day 3
E0.5
on Day 4
E9.5
on Day13
newborn
F
Pooled birth rate
after the injection
%
Birth rate
2x10^5
1x105
5x10^4
2.5x10^4
1x10^4
5x10^3
PBS
Cells / Embryo

Figure 2

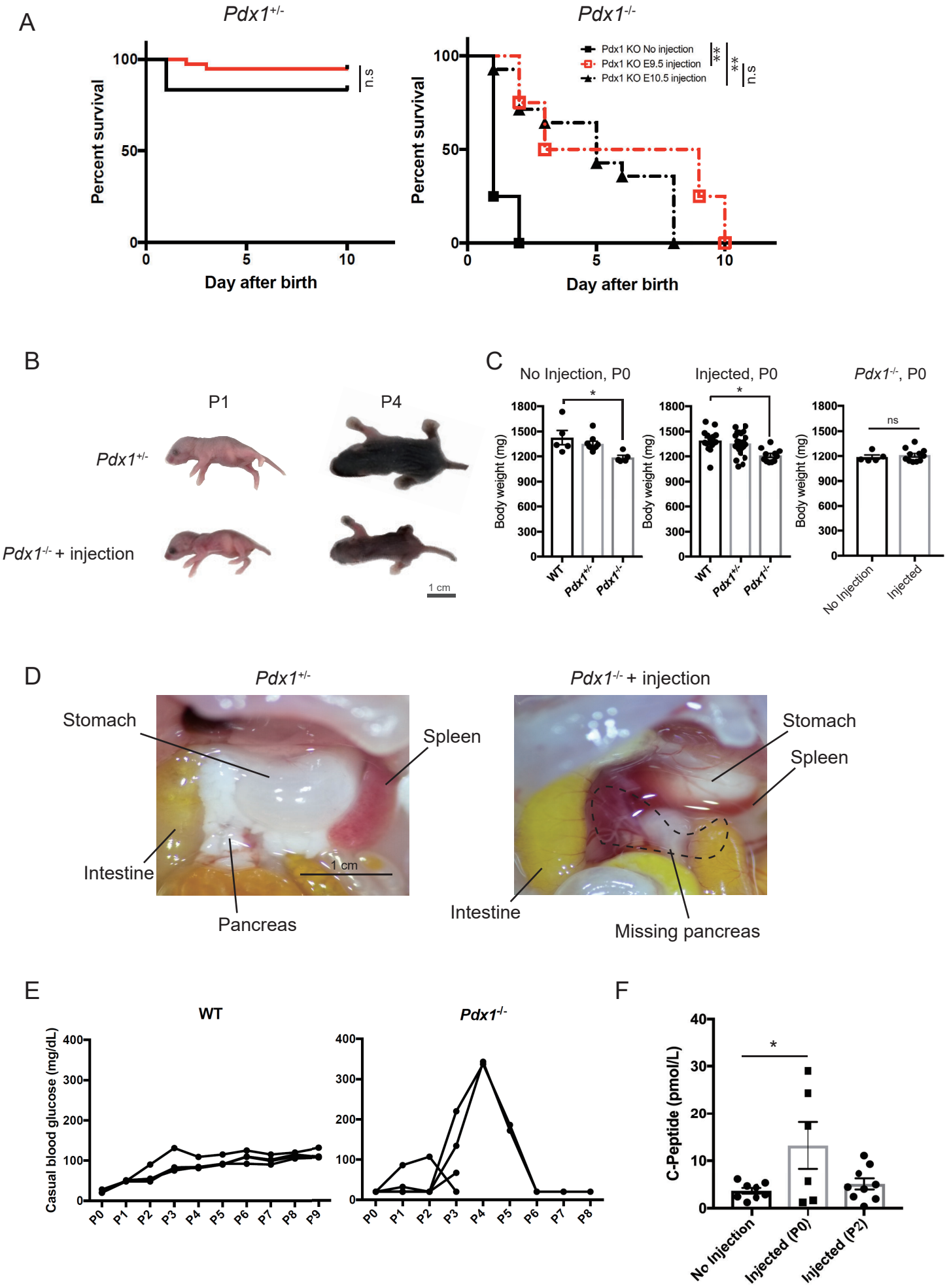
A
Pdx1+/-
Pdx1-/-
Percent survival
Day after birth
n.s
Pdx1 KO No injection
Pdx1 KO E9.5 injection
Pdx1 KO E10.5 injection
**
B
P1
P4
Pdx1+/-
Pdx1-/- + injection
1 cm
C
No Injection, P0
Injected, P0
Pdx1-/-, P0
Body weight (mg)
WT
Pdx1+/-
Pdx1-/-
No Injection
Injected
ns
D
Pdx1+/-
Pdx1-/- + injection
Stomach
Spleen
Intestine
Pancreas
1 cm
Missing pancreas
E
WT
Casual blood glucose (mg/dL)
F
C-Peptide (pmol/L)
No Injection
Injected (P0)
Injected (P2)

Figure 3

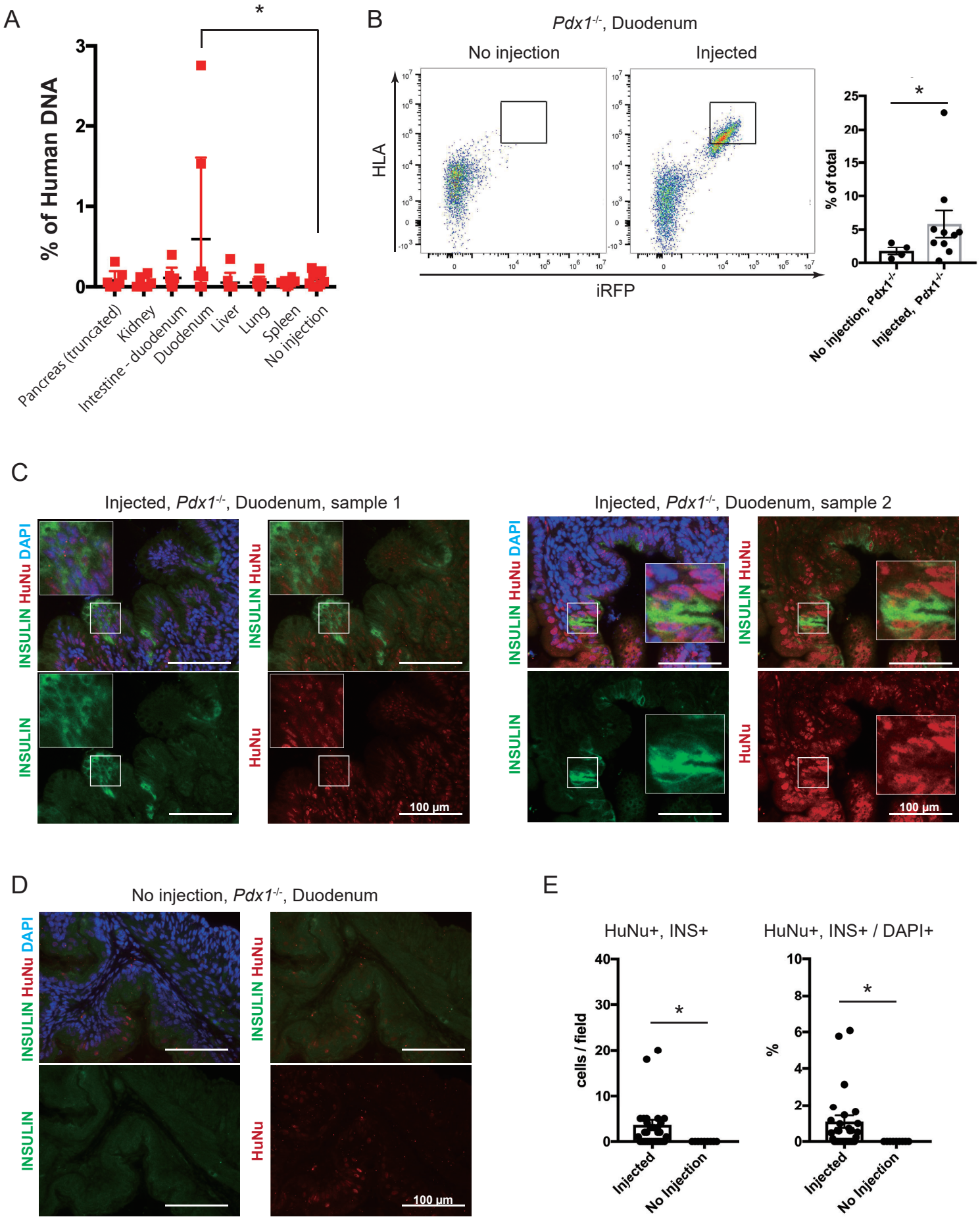
A
% of Human DNA
Pancreas (truncated)
Kidney
Intestine - duodenum
Duodenum
Liver
Lung
Spleen
No injection
B
Pdx1-/-, Duodenum
No injection
Injected
HLA
iRFP
% of total
No injection, Pdx1-/-
Injected, Pdx1-/-
C
Injected, Pdx1-/-, Duodenum, sample 1
Injected, Pdx1-/-, Duodenum, sample 2
INSULIN HuNu DAPI
INSULIN HuNu
INSULIN
HuNu
100 µm
D
No injection, Pdx1-/-, Duodenum
E
HuNu+, INS+
HuNu+, INS+ / DAPI+
cells / field
%
Injected
No Injection

Figure 4

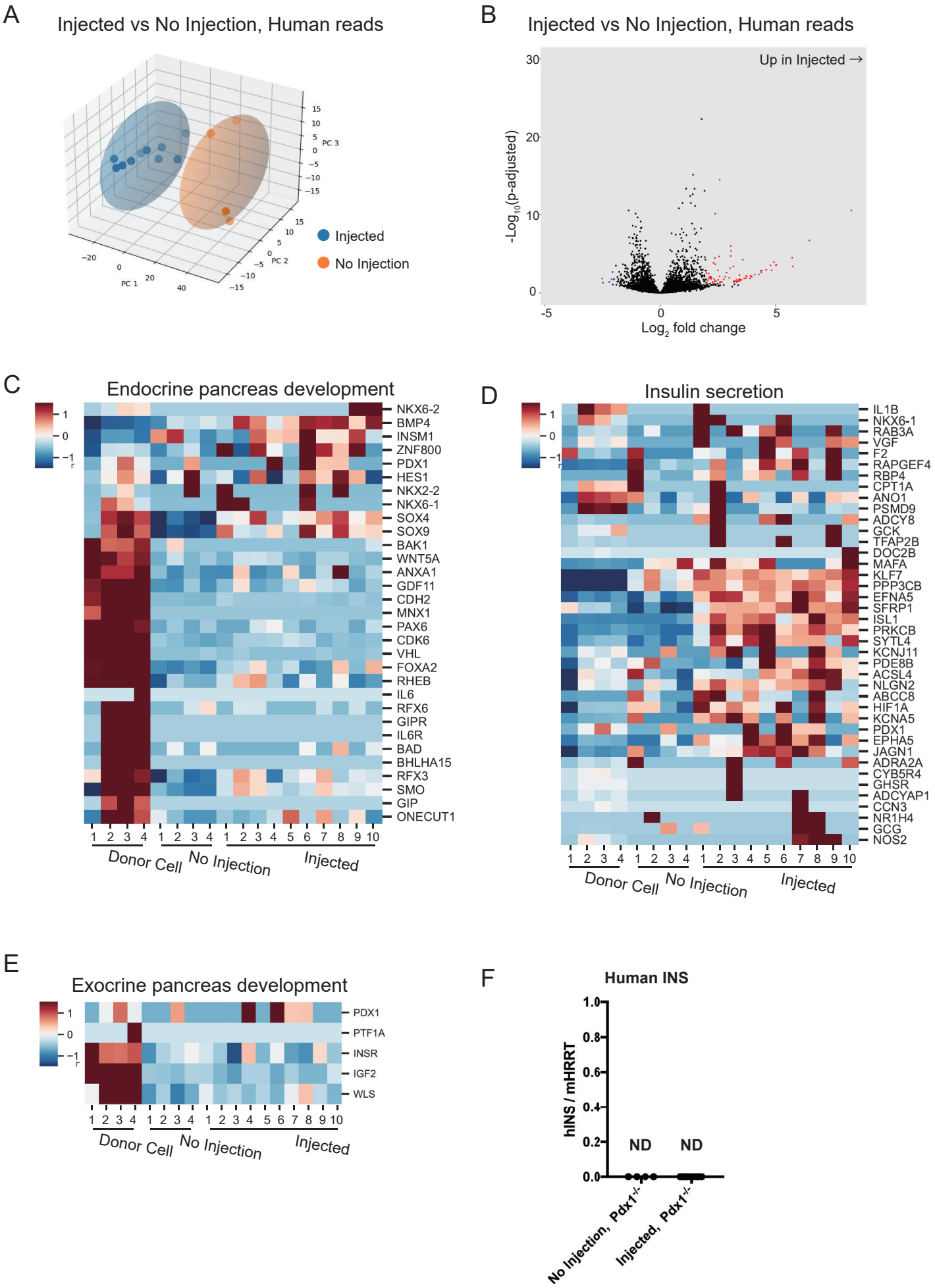
A
Injected vs No Injection, Human reads
PC 1
PC 2
PC 3
Injected
No Injection
B
Injected vs No Injection, Human reads
Up in Injected →
-Log10(p-adjusted)
Log2 fold change
C
Endocrine pancreas development
NKX6-2
BMP4
INSM1
ZNF800
PDX1
HES1
NKX2-2
NKX6-1
SOX4
SOX9
BAK1
WNT5A
ANXA1
GDF11
CDH2
MNX1
PAX6
CDK6
VHL
FOXA2
RHEB
IL6
RFX6
GIPR
IL6R
BAD
BHLHA15
RFX3
SMO
GIP
ONECUT1
Donor Cell
No Injection
Injected
D
Insulin secretion
IL1B
NKX6-1
RAB3A
VGF
F2
RAPGEF4
RBP4
CPT1A
ANO1
PSMD9
ADCY8
GCK
TFAP2B
DOC2B
MAFA
KLF7
PPP3CB
EFNA5
SFRP1
ISL1
PRKCB
SYTL4
KCNJ11
PDE8B
ACSL4
NLGN2
ABCC8
HIF1A
KCNA5
PDX1
EPHA5
JAGN1
ADRA2A
CYB5R4
GHSR
ADCYAP1
CCN3
NR1H4
GCG
NOS2
Donor Cell
No Injection
Injected
E
Exocrine pancreas development
PDX1
PTF1A
INSR
IGF2
WLS
Donor Cell
No Injection
Injected
F
Human INS
hINS / mHRRT
ND
ND
No Injection, Pdx1-/-
Injected, Pdx1-/-